Solid Freeform Fabrication 2021: Proceedings of the 32nd Annual International
Solid Freeform Fabrication Symposium – An Additive Manufacturing Conference
Reviewed Paper

Material characterization of diversely aggregated cementitious materials produced with a modular lightweight additive manufacturing extrusion system

Mehrab Nodehi[1]*, Bahram Asiabanpour[1], Liam Omer[1], Togay Ozbakkaloglu[1]

[1] Ingram School of Engineering, Texas State University, San Marcos, TX 78666, USA

*M_N224@txstate.edu

Abstract

Applications of additive manufacturing in the construction industry started three decades ago with the first patent and prototype of the contour crafting process. Since then, its obvious benefits in reducing labor cost, construction waste while improving efficiency and flexibility have led to the development of several large-scale commercial machines in this field. However, proper lab-scale machines for training experts in automated construction and research-based activities such as material optimizations for civil and structural engineers are not available. The only available small-scale apparatus in AM-based construction is limited to a minimal list of materials and properties. Those machines are not capable of fabricating samples from cementitious materials with a variety of aggregate sizes. This paper compares two low-cost, modular AM-based construction systems capable of extruding a wide variety of cementitious materials with diverse aggregate sizes. The systems are capable of controlled extrusion with a variety of cross-section forms. The system can be attached to a robotic arm, CNC machine, or other programmable machines. As a proof-of-concept, the developed system is utilized to fabricate cement mortar with larger aggregate sizes with different materials mixture ratios. Mechanical performance of the resulting additively manufactured cementitious parts is examined and compared.

Keywords: Additive manufacturing, 3D printing cementitious materials, 3d concrete printing;

1. Introduction

Since the conceptual development of the fourth industrial revolution (Industry 4.0), additive manufacturing (3D printing) has become a vital technology in multiple engineering sectors to align with automation and smartification. In the construction industry, the application of 3D printing has been mostly researched on the production of automated concrete 3D printing to reduce labor costs and obviate the need for formwork. Starting from the introduction of 3D printing in construction by Khoshnevis [1], major attempts have been made to further enhance and discover the unfolded potentials of this newly-born technology (see figure 1). Through recent trials, this technology has shown potential to reduce labor costs, and construction waste up to 50 and 30%, respectively [2]–[4]. Although always seen as beneficial, the printing process and the lack of commonly used formworks and molds in 3D printing concrete (3DPC), significantly increases the difficulty in the printing process. This process, in that respect, includes the extrusion of the cementitious materials which is directly influenced by the fresh properties of the mortar or concrete [5]. Accordingly, rheological properties are the most sensitive and significant properties that can limit the quality of the printed materials. The degree to which rheology contributes to the printing process is in harmony with the printers' designed extruders and nozzles. In other words, the mixture's design should be aligned with the extruder and nozzle's size to be able to effectively print concrete or cementitious materials. On this basis, one of the major issues associated with 3D concrete printing is the materials' roughness and size. Aggregates that affect the overall viscosity of the extrusion process define the potential extrudability, as well as pumpability of the mixture [6]. In addition, viscosity changes are subject to additional binding agents (e.g., cement and supplementary cementitious materials), as well as the size, content, and particle distribution of aggregates.

According to [5], a binding mixture with plastic viscosity equal to (38.7 ±4.5) Pa.s (for CEM I & coal fly ash), and (21.1 ±2.4) Pa.s (for CEM I & limestone filler), were suitable for pumping and extrusion. However, based on the result of [4], [7]–[12], the aggregate size must be between one-fifth (1/5) to one-tenth (1/10) of the actual nozzle orifice (see table 1), for the materials to be printable. This is due to the higher yield stress of finer particles [6] and the ability of the printer to pump the materials from a smaller orifice without nozzle obstruction.

To reduce the possibility of blockage multiple strategies have been adopted within the literature including:

- **Higher contents of cementitious materials:** Due to higher adhesion and higher geometric stability of materials to sustain their shape while supporting the weight of additional layers.
- **Finer aggregate particles**: To provide the mixture with higher yield stress that supports buildability [6].
- **Higher use of admixtures:** admixtures such as high range water reducers, and retarders are most commonly used in 3D concrete printing to elongate the setting time and allow an elongated duration for printing to be performed.
- **Larger orifice nozzles:** Allows for the extrusion of high aggregate size and lower force required for successful extrusion

Due to the relatively high initial costs and complexity of multi-systematic operation of the commonly commercialized (extrusion-based) 3D printers, research and development practices require a larger sum of funding for entertaining this novel technology. As a result, in this study,

we provide a proof-of-concept on utilizing a simple, functional instrument that can meet the expectations of Civil and Structural engineers while also provide a simple means for research and development studies. Unlike most cementitious-materials 3D printers that rely on hydraulic pumps, robotic arms, or air pressures, our system is based on a simplistic screw-based extrusion using gravity-fed material delivery to reduce the need for the additional systems while providing the ability to 3D print cement mortar with larger aggregate sizes. Depending on the filament's viscosity, a gravity-based material feed system, as well as the other mentioned pressurizing system, can be coupled with this novel system obviating the need for costly and large instruments that are commonly commercialized. In accordance, a proof-of-concept with different materials mixture ratios is provided and discussed.

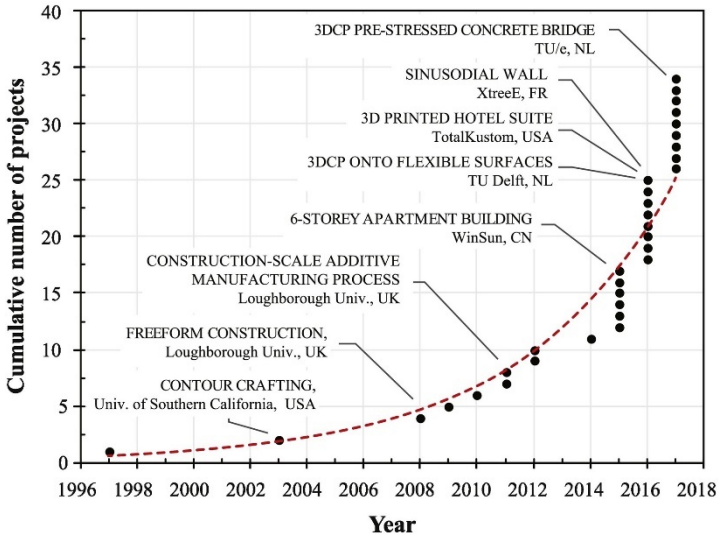

Figure 1: showing the 3D concrete printing progress from late 90s to 2018 [5]

Reference	size of aggregate	Nozzle size	Layer height	Sand:Binder ratio	Max nozzle diameter to agg size ratio
[7]	4.75 mm	25 mm (Circular)	10 mm	1.4	5.2
[8]	0.9 mm	30 mm (Circle)	15 mm	1	33
[13]	1 mm	N/A	8,9.5,11 mm	N/A	N/A
[4]	500 µm	25 mm × 15 mm	N/A	1.5	30
[14]	N/A	30 mm × 15 mm	15 mm	1.2	N/A
[6]	1.18, 2.36, 4.75	N/A	N/A	N/A	N/A
[15]	2 mm	20 mm (Circular)	15 mm	1.5	10
[16]	1.2 mm	30 mm × 15 mm	15 mm	1	12.5
[9]	2 mm	20 × 20 mm	15 mm	1.22	10
[17]	0.25 mm	N/A	N/A	N/A	N/A
[18]	10 mm	N/A	N/A	1.25	N/A
[19]	2 mm	9 mm	N/A	1.5	4.5
[10]	1.18 mm	13 mm × 30 mm	13 mm	1.5	11
[11]	1 mm	20 mm (Circular)	12-15 mm	0.6, 0.8, 1, 1.2, 1.5	20
[20]	N/A	N/A	6mm	1	N/A
[21]	1.15 mm	30×15,20×20 mm	N/A	N/A	13
[22]	4.75 mm	25 mm (Circular)	15 mm	N/A	5.2
[23]	0.2 mm	N/A	N/A	N/A	N/A
[24]	N/A	30×15 mm	15 mm	1.2	N/A
[12]	2 mm	40×13.5 mm	25-27 mm	1.875	6.75

Table 1: reporting the max aggregate size versus that of nozzle dimensions with a successful printing

2. Methodology

For this study, ordinary Portland cement (OPC) conforming to ASTM C150, as well as river sand with an overall particle size distribution (max <5 mm) illustrated in figure 2, was used conforming to ASTM C136. In addition, table 1 outlines the bulk and apparent specific gravity, and total absorption of river sand particles, which was tested based on ASTM C128. Specific material composition for extrudes concrete samples can be seen in Table 3.

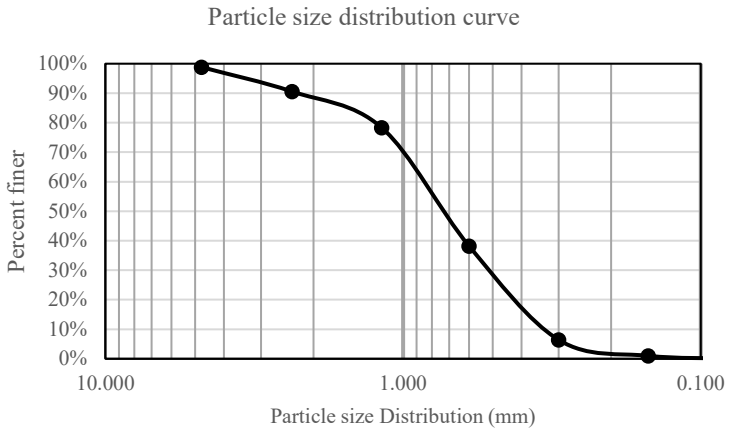

Figure 2: particle size distribution of river sand used.

River sand			
Bulk S.G. (Kg/m3)	Bulk S.G. SSD (Kg/m3)	Apparent S.G. (Kg/m3)	Absorption (%)
2616.4	2667	2755.7	1.93

Table 2: showing the result of ASTM C136, conducted on the river sand as part of this study.

Materials	OPC	RS	Water	Fly ash	GGBFS	SP and retarder (g/l)
Proportion	1	0.5	0.33	0.5	0.5	1.3

Table 3: Outlining the Mixture proportions used for this research

2.1.Instruments

Currently, there are a variety of delivery systems for use within additively manufactured concrete systems. For the scope of this research within concrete extrusion, only fused filament-forming additive manufacturing processes will be discussed. Concrete extrusion systems are

reliant on material mixing, material delivery, and material deposition. Material mixing ensures appropriate dispersion of constituent materials in addition to appropriate hydration. This is often accomplished through mechanical mixing of the materials in paddle or screw mixers that introduce wall shearing and turbulence within the material to disperse aggregates and additives. Material delivery is usually accomplished through gravity fed or pump-assisted systems. Gravity-fed systems essential create pumping pressure through potential energy provided by the height of the material reservoir being above the deposition head. Gravity fed systems provide a simple and cost-effective method for delivering cementitious materials that only require energy to raise the reservoir to appropriate heights. A pump-assisted system used hydraulic rams to mechanically press materials through either piping or high pressure hoses to the deposition head. The advantages to pumping systems are volumetric flow control and material resevoirs at ground level. However, pump systems are inherently expensive due to their hydraulic force systems that include precision rams, motors, manifolds, and high pressure hoses. In addition, these systems are intended for construction applications that require large volumes of concrete at a given time. The large volume systems are not conducive to small batch experimentation with exploratory additives such a geopolymer and would produce significantly larger amounts of waste than gravity-filled canisters. With cost-effectiveness and ease of use in mind, a gravity-fed canister was used to deliver material to the screw-based extrusion mechanism presented in this paper. It provides material delivery without the need for power while also providing an opportunity to continuously fill the reservoir during additive manufacturing of large-scale parts.

Lutum V4

The Lutum V4 is an all-in-one, extrusion-based instrument that is designed for the additive manufacture of clay-based materials. As a part of this study, to provide further insight on the extrudability of different mixes and materials for further comparison, 18 mixes were designed and attempted. Printing success is documented in table 4. Due to the small auger orifice, the system was unable to print cementitious materials with large aggregate sizes common in state-of-the-art concretes. Although this system provides the ability to print controlled geometries using an auger-based delivery system, its cost and small orifice limit its use in experimental concrete construction or experimentation.

2.1.1. Piston-based extrusion

Another instrument used to additively manufacture (3D printing) cementitious materials is a piston-based extrusion mechanism, supplied from locally available markets. Having major similarities to the adhesive containers used in [132], it can keep cementitious materials within and based on the nozzle of choice, extrude the material through the mechanical force of the rearward piston. The design illustrated below used an additively manufactured thermoplastic die that can be interchanged with other dies to obtain a variety of different nozzle sizes and shapes. The device provides an affordable method for producing extruded concretes samples for testing in standard industry ASTM mechanical testing. In addition, the use of dies additively manufactured using readily available polylactic acid thermoplastic allows users to manipulate die form without the use of machining or tooling.

Materials used	Sand	Water	Additive	Max aggregate size	Nozzle size	Printable?
OPC: 1	-	-	-	-	1 mm	No
OPC: 1	-	-	-	600 μm	1 mm	No
OPC: 1	-	-	-	-	7 mm	Yes
OPC: 1	-	-	-	600 μm	7 mm	Yes
OPC: 1	RS: 1	-	-	2 mm	7 mm	Partially
OPC: 1	RS: 0.5	-	-	2 mm	7 mm	Yes
OPC: 1	RS: 1	-	-	4.75 mm	7 mm	No
OPC: 1	RS: 1	-	-	2 mm	10 mm	Yes
OPC: 1	RS: 1	-	-	2 mm	7 mm	No
0.5 OPC – 0.5 FA (C)	-	-	-	4.75 mm	7 mm	No
0.5 OPC – 0.5 FA (C)	-	-	-	2 mm	10 mm	Partially
0.5 OPC – 0.25 FA (C) – 0.25 GGBFS	-	-	-	+4.75 mm	20 x 10 mm (90˚)	No
0.5 OPC – 0.5 GGBFS	-	-	-	2 mm	20 x 10 mm (90˚)	No
OPC: 1	RS: 1	W: 0.35	SP 0.007 RET: 0.012	2 mm	20 x 10 mm (90˚)	No
OPC: 1	RS: 1	W: 0.30	SP 0.007 RET: 0.012	2 mm	20 x 10 mm (90˚)	No
OPC: 1	RS: 1	W: 0.30	RET: 0.012	2 mm	20 x 10 mm (90˚)	No
OPC: 1	RS: 1	W: 0.30	-	1 mm	20 mm spherical	No
OPC 2	RS: 1	W: 0.37	RET: 0.025	1 mm	20 mm spherical	No

Table 4: representing the trials conducted with different mixes and different nozzle sizes (with OPC: Ordinary Portland Cement, FA: coal fly ash, GGBFS: Ground granulated blast furnace slag, RS: river sand, W: water, SP: superplasticizer, and RET: retarder)

Mechanically Actuated Piston Extruder	
	

Mixture										
FA	GGBFS	NaOH	Molarity	OPC	SP & RT (g/L)	Water	R.S.	Max ag. size (mm)	Nozzle size (mm)	Printable?
0.5	0.5	0.398	12	-	-	-	1	2	30×7	High slump
0.5	0.7	0.398	12	-	-	-	1	2	30×7	Yes
-	1	0.398	12	-	-	-	1	2	30×7	Yes
1	-	-	-	1	1.3	0.33	0.5	2	30× 10	Yes
1	-	-	-	1	2.6	0.33	0.5	2	30× 10	Yes
1	-	-	-	1	9.08	0.33	0.5	2	30× 10	Yes
1	-	-	-	1	9.08	0.291.5	0.5	2	30× 10	Yes
1	-	-	-	1	9.73	0.262	0.5	2	30× 10	Yes

Table 5: Outlining the mixture ratios utilized to experiment with the piston extruder (SP stands for superplasticizer and RT refers to retarder.

Using the modified piston extruder, as shown in figure 7, geopolymer mortar with sodium hydroxide (12M) used as an activator has been successfully printed.

Figure 3: Illustration of 3D printed concrete with piston extruder using a variety of modified nozzles additively manufactured with fused filament-forming polylactic acid.

2.1.2. Auger Screw Extrusion

Screw-based extrusion is a heavily used technique for the extrusion of high viscosity materials such as polymers, composites, and cements. The advantages of the screw-based extrusion system are multifold. The extrusion screw can be refilled continuously, the rotary motion of the screw can provide aggregate dispersion, and extrusion and retraction are possible. Based on this experiment, the use of a continuous extrusion system has been a major success whereby cement mortar has been successfully additively manufactured without any constraints on aggregate size.

Auger Screw Based Extrusion

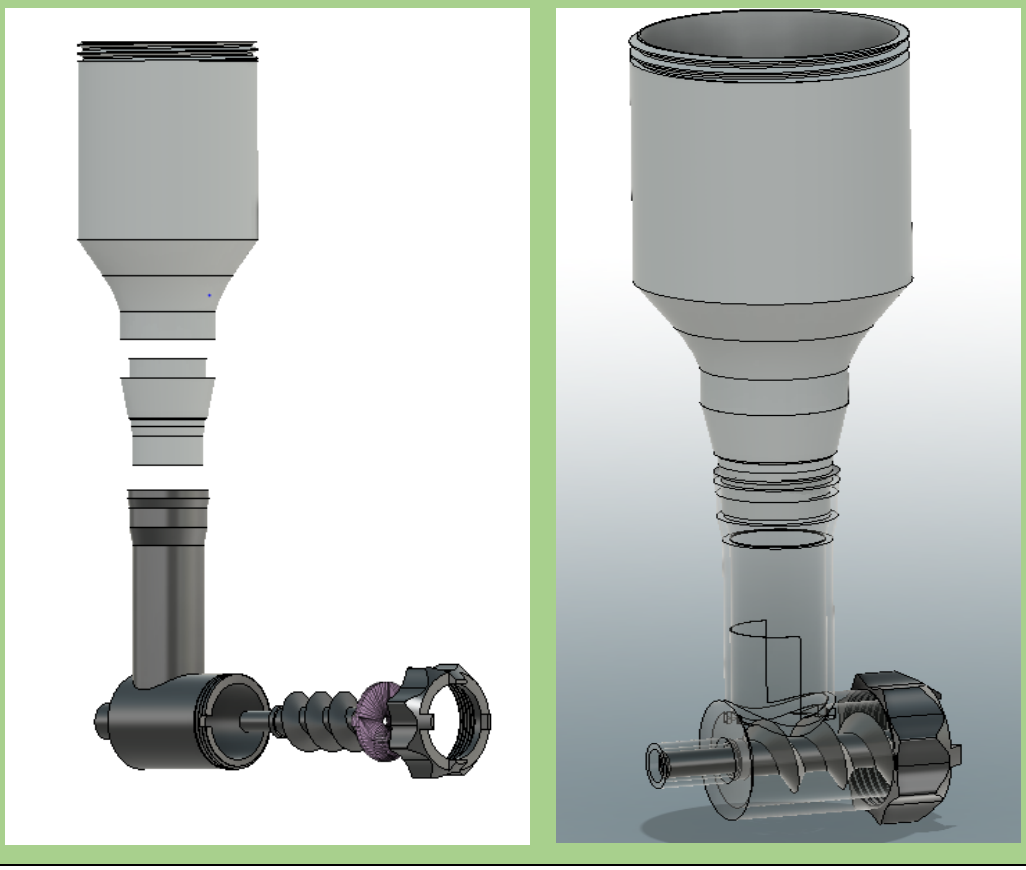

OPC	FA	GGBFS	Water	SP & RT (g/L)	Aggregate	Max aggregate size (mm)	Nozzle size (mm)	Printable?
1	0.5	0.5	0.33	1.3	0.5	2	30×7	Yes
1	0.5	0.5	0.33	2.6	0.5	2	30×7	Yes
1	1	-	0.33	2.6	0.5	2	30×7	Yes
1	1	-	0.291.5	9.08	0.5	2	30×7	Yes
1	1	-	0.262	9.08	0.5	2	30×7	Yes
1	1	-	0.25	9.73	0.5	2	30×7	Yes

Table 6: showing the mixture proportions used for experimenting with the screw based extrusion system

1. Sample Curing

After the specimens were printed, they were placed in a curing room with an ambient temperature of 23 ˚C (+2 or -2), with a relative humidity of 50% (+2 or -2), conforming to ASTM C109 until tested.

3. Results

3.1. Fresh Property Test – Flow Properties

To test the fresh property of the mortar, the flow table, a common testing instrument used in self-compacting concrete and mortar testing has been adopted, conforming to ASTM C1437 [74]. Based on the result of the flow table, the mixture had a spread diameter of 165 mm.

Figure 4: Showing the result of flow table test, conforming to ASTM C1437.

3.2. Compressive strength

To measure the compressive strength of printed materials, specimens with the size of 20×20 mm were sawn from larger printed samples. Specimen were then put in Automax compression testing machine according to ASTM C109 under load control at the rate of 25 MPa/min as in [11]. Based on figure 5, screw-based specimen had a relatively higher compressive strength. This can be attributed to better material dispersion in presence of an auger that results in enhanced hydration of cementitious materials.

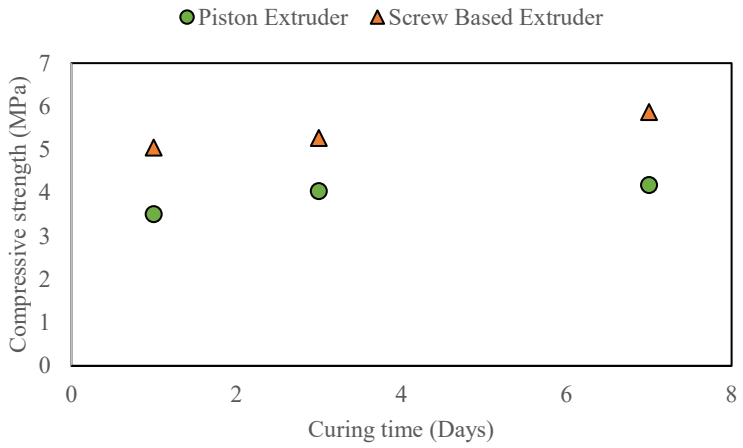

Figure 5: Showing the result of compressive strength test (ASTM C109) conducted on the printed specimen by screw-based system compared to piston based extruder

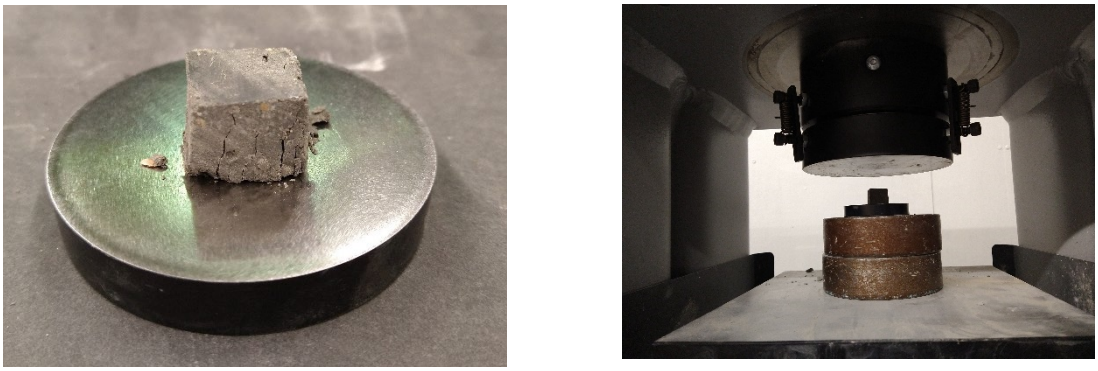

Figure 6: from left, showing the type of failure of cube specimen and its position prior to the compression test

3.3. Flexural strength

For testing flexural strength of the specimen, based on the printed materials specimen with the size of 40 mm × 135 mm were sawn and put under a flexural testing machine with load rating conforming to ASTM C109. Based on figure 7, the piston-based extruder samples had a relatively higher flexural strength which can be attributed to a lower number of layers, resulting in potentially reduced inter-layer porosity.

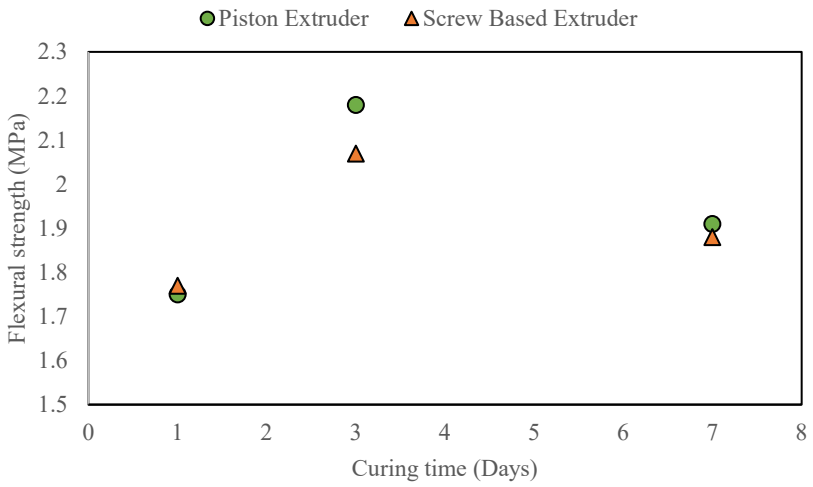

Figure 7: Showing the result of flexural strength test (ASTM C109) conducted on the printed specimen by screw-based system compared to piston based extruder

Figure 8: Failure under flexural strength test for specimen printed by piston based extruder (left) and auger screw based extruder system (on the right)

4. **Sample Quality**

Although the piston-based extrusion mechanism provided a low-cost mechanism for concrete extrusion, it was noted that the dispersion of the resulting extrusions was poor. This is likely due to the settling of aggregates out of the mortar due to the absence of any mixing action. In addition, the piston-based extrusion is constrained by its container size. The mechanism is only capable of extruding its reservoirs volume at a time before requiring disassembly for material replenishment. This discontinuous system is capable of providing small samples for material characterization, but would not be suitable for additive manufacturing of concretes.

Due to the piston extrusion samples having larger layer height, larger drying shrinkage cracks were observed in comparison to screw extruder samples. Additionally, samples experienced a relatively large number of micro-pores and air-void pores which may be due to lack of vibration as compared to conventionally casted concrete.

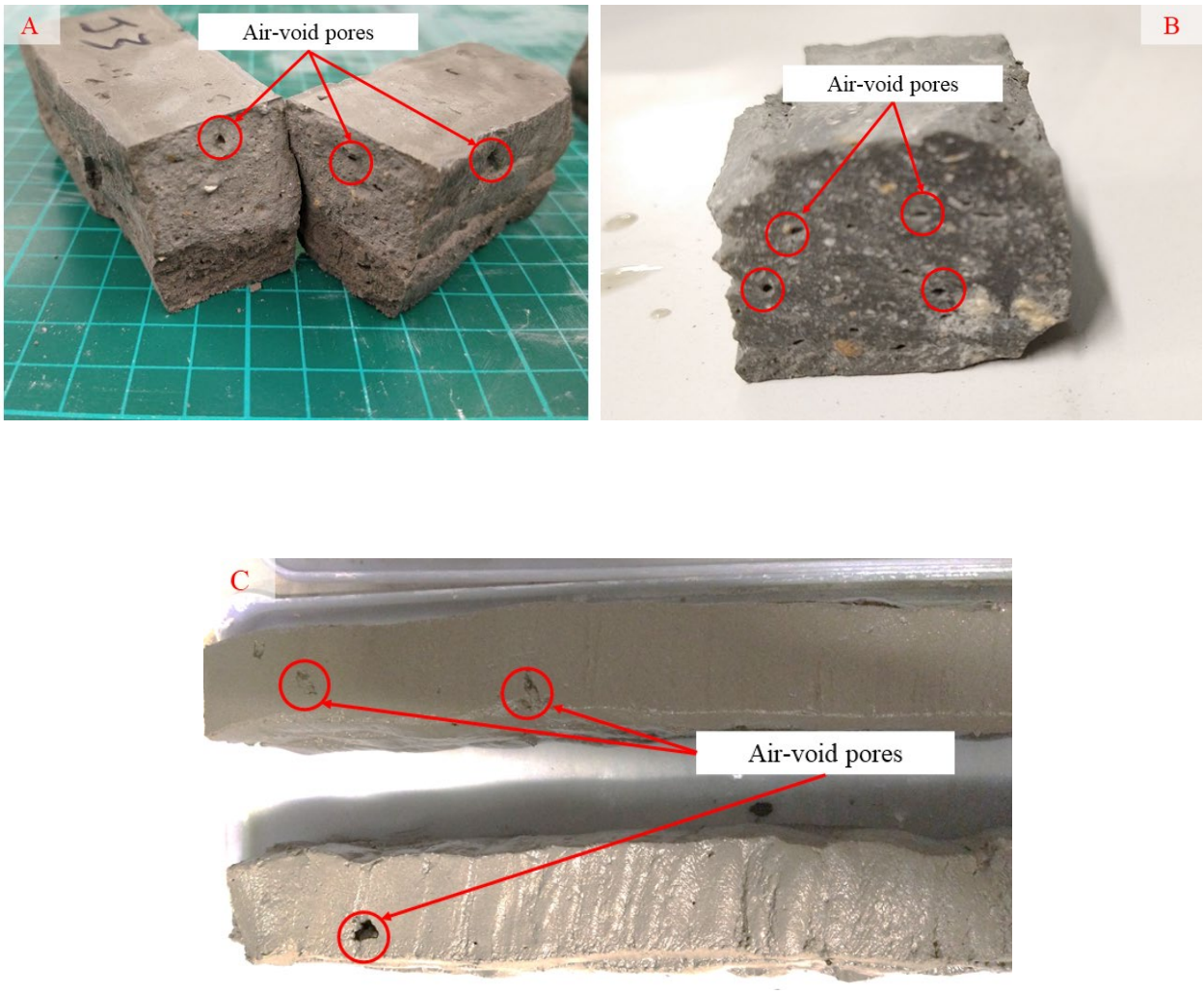

Figure 9: Void Formation within extruded samples

5. Conclusion and discussion

In general, to 3D print cementitious materials, there are a few challenges that should first be addressed. The material set time of the mixture, viscosity, and aggregate size are vital factors to achieve successful printing. Based on previous studies, a ratio of nozzle diameter to the aggregate size of 1:5 is an ideal approach to prevent nozzle obstruction during extrusion. Successful results of printed samples and the mechanical

property tests support the use of the introduced modular lightweight additive manufacturing system for 3D printing cementitious materials based on screw-based extrusion using simple to create thermoplastic dies. The system provides a simply designed extruder for mounting onto gantry or robotic arms for automated printing. As in any other additive manufacturing technique, an automated process is expected to take place which, in most 3D printing cementitious materials is conducted through a control arm. In our auger screw extrusion system, although it has been used in absence of an automated arm, it clearly shows potential for a constant feeding system connected to an automated control arm. Further experimentation is required to hone the linear advance, extrusion rates, and slicing associated with the automated printing using this low-cost alternative.

6. Acknowledgment

The authors cordially appreciate the use of the Texas State University Ingram Hall Makerspace in providing both expertise and machinery for producing our prototypes. In addition, we appreciate Texas State University providing the ground for our educational exploration with the freedom to develop new and interesting ideas.

7. References

[1] B. Khoshnevis, "Automated construction by contour crafting - Related robotics and information technologies," *Autom. Constr.*, vol. 13, no. 1, pp. 5–19, 2004, doi: 10.1016/j.autcon.2003.08.012.

[2] J. Zhang, J. Wang, S. Dong, X. Yu, and B. Han, "A review of the current progress and application of 3D printed concrete," *Compos. Part A Appl. Sci. Manuf.*, vol. 125, no. April, p. 105533, 2019, doi: 10.1016/j.compositesa.2019.105533.

[3] V. Mechtcherine *et al.*, "Integrating reinforcement in digital fabrication with concrete: A review and classification framework," *Cem. Concr. Compos.*, p. 103964, 2021, doi: 10.1016/j.cemconcomp.2021.103964.

[4] J. G. Sanjayan, B. Nematollahi, M. Xia, and T. Marchment, “Effect of surface moisture on inter-layer strength of 3D printed concrete,” *Constr. Build. Mater.*, vol. 172, pp. 468–475, 2018, doi: 10.1016/j.conbuildmat.2018.03.232.

[5] R. A. Buswell, W. R. Leal de Silva, S. Z. Jones, and J. Dirrenberger, “3D printing using concrete extrusion: A roadmap for research,” *Cem. Concr. Res.*, vol. 112, no. June, pp. 37–49, 2018, doi: 10.1016/j.cemconres.2018.05.006.

[6] C. Zhang, Z. Hou, C. Chen, Y. Zhang, V. Mechtcherine, and Z. Sun, “Design of 3D printable concrete based on the relationship between flowability of cement paste and optimum aggregate content,” *Cem. Concr. Compos.*, vol. 104, no. September, p. 103406, 2019, doi: 10.1016/j.cemconcomp.2019.103406.

[7] G. M. Moelich, J. Kruger, and R. Combrinck, “Plastic shrinkage cracking in 3D printed concrete,” *Compos. Part B Eng.*, vol. 200, no. July, p. 108313, 2020, doi: 10.1016/j.compositesb.2020.108313.

[8] T. Ding, J. Xiao, S. Zou, and Y. Wang, “Hardened properties of layered 3D printed concrete with recycled sand,” *Cem. Concr. Compos.*, vol. 113, no. June, p. 103724, 2020, doi: 10.1016/j.cemconcomp.2020.103724.

[9] B. Panda, N. A. N. Mohamed, S. C. Paul, G. V. P. B. Singh, M. J. Tan, and B. Šavija, “The effect of material fresh properties and process parameters on buildability and interlayer adhesion of 3D printed concrete,” *Materials (Basel).*, vol. 12, no. 13, 2019, doi: 10.3390/ma12132149.

[10] J. H. Lim, B. Panda, and Q. C. Pham, “Improving flexural characteristics of 3D printed geopolymer composites with in-process steel cable reinforcement,” *Constr. Build. Mater.*, vol. 178, pp. 32–41, 2018, doi: 10.1016/j.conbuildmat.2018.05.010.

[11] Y. Zhang, Y. Zhang, W. She, L. Yang, G. Liu, and Y. Yang, “Rheological and harden properties

of the high-thixotropy 3D printing concrete," *Constr. Build. Mater.*, vol. 201, pp. 278–285, 2019, doi: 10.1016/j.conbuildmat.2018.12.061.

[12] Y. Chen *et al.*, "Effect of printing parameters on interlayer bond strength of 3D printed limestone-calcined clay-based cementitious materials: An experimental and numerical study," *Constr. Build. Mater.*, vol. 262, 2020, doi: 10.1016/j.conbuildmat.2020.120094.

[13] R. J. M. Wolfs, F. P. Bos, and T. A. M. Salet, "Hardened properties of 3D printed concrete: The influence of process parameters on interlayer adhesion," *Cem. Concr. Res.*, vol. 119, no. January, pp. 132–140, 2019, doi: 10.1016/j.cemconres.2019.02.017.

[14] Y. W. D. Tay, G. H. A. Ting, Y. Qian, B. Panda, L. He, and M. J. Tan, "Time gap effect on bond strength of 3D-printed concrete," *Virtual Phys. Prototyp.*, vol. 14, no. 1, pp. 104–113, 2019, doi: 10.1080/17452759.2018.1500420.

[15] K. Federowicz, M. Kaszyńska, A. Zieliński, and M. Hoffmann, "Effect of curing methods on shrinkage development in 3D-printed concrete," *Materials (Basel).*, vol. 13, no. 11, 2020, doi: 10.3390/ma13112590.

[16] T. Ding, J. Xiao, S. Zou, and X. Zhou, "Anisotropic behavior in bending of 3D printed concrete reinforced with fibers," *Compos. Struct.*, vol. 254, no. July, p. 112808, 2020, doi: 10.1016/j.compstruct.2020.112808.

[17] L. Wang, H. Jiang, Z. Li, and G. Ma, "Mechanical behaviors of 3D printed lightweight concrete structure with hollow section," *Arch. Civ. Mech. Eng.*, vol. 20, no. 1, pp. 1–17, 2020, doi: 10.1007/s43452-020-00017-1.

[18] Y. Ju *et al.*, "Visualization of the three-dimensional structure and stress field of aggregated concrete materials through 3D printing and frozen-stress techniques," *Constr. Build. Mater.*, vol. 143, pp. 121–137, 2017, doi: 10.1016/j.conbuildmat.2017.03.102.

[19] T. T. Le *et al.*, “Hardened properties of high-performance printing concrete,” *Cem. Concr. Res.*, vol. 42, no. 3, pp. 558–566, 2012, doi: 10.1016/j.cemconres.2011.12.003.

[20] L. Pham, P. Tran, and J. Sanjayan, “Steel fibres reinforced 3D printed concrete: Influence of fibre sizes on mechanical performance,” *Constr. Build. Mater.*, vol. 250, p. 118785, 2020, doi: 10.1016/j.conbuildmat.2020.118785.

[21] B. Panda, S. C. Paul, N. A. N. Mohamed, Y. W. D. Tay, and M. J. Tan, “Measurement of tensile bond strength of 3D printed geopolymer mortar,” *Meas. J. Int. Meas. Confed.*, vol. 113, no. September 2017, pp. 108–116, 2018, doi: 10.1016/j.measurement.2017.08.051.

[22] A. Cicione, J. Kruger, R. S. Walls, and G. Van Zijl, “An experimental study of the behavior of 3D printed concrete at elevated temperatures,” *Fire Saf. J.*, no. January, p. 103075, 2020, doi: 10.1016/j.firesaf.2020.103075.

[23] C. Joh, J. Lee, T. Q. Bui, J. Park, and I.-H. Yang, “Buildability and Mechanical Properties of 3D Printed Concrete,” *Materials (Basel).*, vol. 13, no. 21, p. 4919, Nov. 2020, doi: 10.3390/ma13214919.

[24] G. H. A. Ting, Y. W. D. Tay, Y. Qian, and M. J. Tan, “Utilization of recycled glass for 3D concrete printing: rheological and mechanical properties,” *J. Mater. Cycles Waste Manag.*, vol. 21, no. 4, pp. 994–1003, 2019, doi: 10.1007/s10163-019-00857-x.

[25] A. S. Alchaar and A. K. Al-Tamimi, “Mechanical properties of 3D printed concrete in hot temperatures,” *Constr. Build. Mater.*, vol. 266, p. 120991, 2021, doi: 10.1016/j.conbuildmat.2020.120991.